Original Article

Check for updates

Available online at
www.heca-analitika.com/ljes

Leuser Journal of Environmental Studies

Vol. 1, No. 1, 2023

Utilization of Drone with Thermal Camera in Mapping Digital Elevation Model for Ie Seu'um Geothermal Manifestation Exploration Security

Ridzky Aulia Bahri [1], Teuku Rizky Noviandy [1], Rivansyah Suhendra [2], Ghazi Mauer Idroes [3], Muhammad Yanis [4], Erkata Yandri [5], Nizamuddin Nizamuddin [1] and Irvanizam Irvanizam [1]

[1] Department of Informatics, Faculty of Mathematics and Natural Sciences, Universitas Syiah Kuala, Banda Aceh, 23111, Indonesia; ikiabahry@gmail.com (R.A.B.); trizkynoviandy@gmail.com (T.R.N.); niz4muddin@unsyiah.ac.id (N.N.); irvanizam.zamanhuri@usk.ac.id (I.I.)
[2] Department of Information Technology, Faculty of Engineering, Universitas Teuku Umar, Aceh Barat, 23681, Indonesia; rivansyahsuhendra@utu.ac.id (R.S.)
[3] Department of Occupational Health and Safety, Faculty of Health Sciences, Universitas Abulyatama, Aceh Besar 23372, Indonesia; idroesghazi_k3@abulyatama.ac.id (G.M.I.)
[4] Department of Geophysical Engineering, Faculty of Engineering, Universitas Syiah Kuala, Banda Aceh, 23111, Indonesia; yanis@unsyiah.ac.id (M.Y.)
[5] Graduate School of Renewable Energy, Darma Persada University, East Jakarta, 13450, Indonesia; erkata@gmail.com (E.Y.)

***** Correspondence: irvanizam.zamanhuri@usk.ac.id

Article History

Received 24 May 2023
Revised 18 June 2023
Accepted 30 June 2023
Available Online 5 July 2023

Keywords:
Digital elevated model
Drone
FLIR
Geothermal
Temperature

Abstract

Geothermal energy is a viable alternative energy source, particularly in Indonesia. This study was conducted at Ie Seu'um, Mount Seulawah Agam, which is a potential site for a geothermal power plant with an estimated electrical output of 150 megawatts. The objective of this study was to analyze and construct a digital elevation model (DEM) map of the geothermal manifestations. We analyzed water temperature, FLIR (Forward Looking Infrared) temperature, and temperature data from Landsat 8 satellite imagery. To map the heat signature of geothermal features, we utilized the DJI Phantom 4 Standard equipped with the FLIR One Gen 2 sensor. Additionally, we used the Milwaukee Mi306 to calculate the water temperature. Each test was conducted three times to obtain an optimal average level of accuracy. The DEM map was created to assess the level of safety in geothermal manifestation exploration. Elevation and slope values were analyzed to generate a 3D map display, providing a clearer image of the research site. In conclusion, drones prove to be an excellent method for ensuring the safety of exploration in geothermal manifestation areas.

1. Introduction

Many countries attempt to decrease carbon dioxide emissions in the atmosphere by utilizing less fossil fuel as an energy source due to climate change and other environmental issues. One of the most suitable renewable energy techniques is moving away from fossil fuels [1]. Due to its favorable geological conditions, Indonesia is one of the promising countries with abundant renewable energy resources, such as geothermal [2–6]. Currently, Indonesia is in the region of the world's tectonic framework, which is closely related to the potential of geothermal energy. Indonesia has an immense geothermal energy potential, 40% of the world's potential. The potential for geothermal energy in Indonesia is spread over 265 locations along the volcanic

route that stretches from the islands of Sumatra, Java, Bali, Nusa Tenggara, Sulawesi, and Maluku. The data was taken based on the Geological Agency in 2011, with the potential for geothermal power plants in Indonesia at around 29,308 MW [7].

Today, along with the times, especially in the field of information technology, a lot of research is being done to encourage the birth of new discoveries [8]. One of these new discoveries was born is Geographic Information System (GIS) [9]. GIS is a computer information system that can be used to store, manage and analyze, as well as retrieve data with geographic references, which has developed rapidly in the last ten years. The benefits of GIS can be seen from its use in providing convenience for users or decision makers in determining policies, especially those related to spatial aspects, so that this technology will be easy to use for mapping an area, such as a geothermal area [9].

Currently, Indonesia is in the area of the world's tectonic framework and is closely related to the potential of geothermal energy. Geothermal energy locations are sources of renewable energy in the form of heat (thermal) energy that is generated and stored in the earth's core [10].

In GIS, information about the elevation of a surface is a fundamental element of geospatial data used by most users. Height data is usually used for several applications in mapping, such as mapping flood inundation areas, regional planning, road network planning, irrigation network planning, and others. Elevation data is generally stored in a digital elevation model (DEM). DEM is a digital model that represents the shape of the earth's surface in 3D (three dimensions) [11].

Currently, one way that can be done in effective and efficient data collection in GIS is to use flying machines that can be controlled remotely by pilots or can even fly according to the flight plan (autopilot). The glyph is known as Drone or Unmanned Aerial Vehicle (UAV). A drone equipped with a precision navigation wave control system known as GPS (Ground Positioning System). This GPS system is connected to the drone on the electronics flight control- to be able to fly according to the flight plan (autopilot) [12].

The latest terminology of UAV photogrammetry, mapping techniques through aerial photographs explains that drones can be remotely operated and controlled either semi-automatically or automatically without requiring a pilot to sit in. A drone has the capability to carry out photogrammetric measurements, both for measuring areas on a small scale or on a large scale using a photo camera, video camera, thermal, infrared camera, as well as a LiDAR (Light Detection and Ranging) system, or a combination of these. Current UAV standards allow the machine to track the position, as well as the orientation of sensors implemented in a local or global coordinate system. Therefore, this photogrammetric UAV technology can be called the newest photogrammetric measurement tool [13].

Recently, LiDAR systems have become a powerful way to generate maps with DEM models because it has the advantage of gathering 3D information effectively over large areas through precision and timing. However, it should be noted that the main drawback of this drone is its high cost, especially for use in a small study area [14].

In recent years, drones are increasingly being used as a means of observing geothermal manifestations, especially in complex areas such as wetlands, shrubs, steep slopes, and various other conditions in the survey area [15–18]. Using drones, site surveys can be carried out quickly and safely, so this method can ensure researchers' safety [19]. In a study conducted by Marwan et al. [20], it is known that between FLIR One and MAPIR based on processing the data obtained, NDVI from MAPIR shows the research area does not detect temperature well, while thermal data from FLIR shows high temperatures and can detect geothermal manifestations and warm soil. Therefore, in this study, we used the FLIR One thermal camera combined with a drone to explore geothermal energy sources and obtain an estimated surface temperature value from geothermal manifestations. Based on the exploration results, we have also built several DEM maps that can help secure the exploration of the Ie Seu'um geothermal manifestation.

This paper makes several important contributions. Firstly, it creates a Digital Elevation Model (DEM) of Ie Seu'um geothermal manifestations. Secondly, it provides up-to-date information on the safety of exploration areas. Lastly, it conducts research on map usage, specifically focusing on the DEM for ensuring the safety of geothermal manifestation exploration in Ie Seu'um.

This study addresses three main gaps in the current understanding of Ie Seu'um geothermal manifestations. Firstly, it seeks to develop maps and DEM specifically tailored to this geothermal manifestation, which needs improvement. Secondly, it aims to gather information concerning the safety of the exploration area for Ie Seu'um geothermal manifestations, where no such data is currently available. Lastly, the study aims to fill the research gap by investigating the potential use and effectiveness of DEM maps for ensuring the safe exploration of Ie Seu'um geothermal manifestations. This

(a) (b) (c)

Figure 1. Thermal features at the survey site.

area has yet to be explored previously. The study intends to contribute significant knowledge and insights to the field by addressing these gaps.

In this study, to obtain temperature data from water, a temperature measuring device called Milwaukee Mi306, where in its application, this tool is embedded in thermal features, and after that, information about the temperature in the water will be obtained through the monitor. As for elevation data for the Ie Seu'um area, data were obtained from the National DEM website (DEMNAS) to detect peaks and see the height of each test point in this study. Water temperature data will be compared with data obtained from the FLIR thermal camera and satellite imagery data to see which value is the most optimal to use as a reference for research at the location of Ie Seu'um geothermal manifestations.

2. Materials and Methods

2.1. Hardware and Software

The hardware used included a laptop, a DJI Phantom 4 Standard drone, FLIR One Gen 2, GPS Map 62s, Milwaukee Mi306, and an Android smartphone. The software utilized to support the mentioned hardware were Avenza Maps, SAS Planet, FLIR One, ArcMap 10.5, and ArcScene 10.5.

2.2. Data Collection

Data collection was carried out in Ie Seu'um, a geothermal manifestation located in the northern zone of Mount Seulawah Agam, Aceh Besar District, Aceh Province, Indonesia. The collected water temperature was measured directly at the study site using a Milwaukee Mi306. The surface temperature was obtained using a FLIR One Gen 2 connected to the Xiaomi Redmi 3 smartphone, and both devices were linked to the DJI Phantom 4 Standard drone. The data taken when FLIR is flown by drone is in the form of thermal images equipped with temperature information (°C). This temperature is compared with the temperature data in the satellite imagery. The satellite image used is a Landsat 8 satellite image obtained through the USGS Earth Explorer website. The Landsat 8 was used in Collection 1 Level-1 on May 21, 2019, to validate thermal data. Landsat 8 has an image resolution of 100 m for its thermal band. The data used on that date is because we need data with minimal cloud appearance so that in analyzing image temperature data, the results obtained are not the results of surface temperatures blocked by clouds. Landsat 8 consists of five Visual Near Infrared (VNIR) bands (30m resolution), two Short Wave Infrared (SWIR) bands (30m resolution), one panchromatic band (15 m resolution), one band for cirrus cloud detection (30 m resolution), and two Thermal Infrared (TIR) bands (100 m resolution). To obtain NDVI (Normalized Difference Vegetation Index) and surface temperature, data from optical images must go through several essential processing steps, including radiometric correction, brightness temperature calculation, and emissivity calculation. The DEM data in this study uses data from the DEMNAS to determine the value of altitude and peak.

Location coordinates refer to research by [2]. However, in this study, the sample locations were at slightly different coordinate locations. The location of the coordinates can be seen in Table 1. where the table contains three sample points for the location of the Ie Seu'um geothermal manifestation. The thermal features of each site can be seen in Figure 1.

2.3. Data Analysis

Data was analyzed to find differences in values between water temperature, FLIR temperature, and temperature on Landsat 8 satellite imagery. As for elevation data, the analysis was carried out to detect land heights obtained from DEMNAS. For FLIR imagery, data analysis was carried out by analyzing FLIR video recordings when

Table 1. Sample locations in the survey area.

Location	Coordinates	
	N	E
IS1	5°32'50.62"	95°32'55.15"
IS2	5°32'50.08"	95°32'55.29"
IS3	5°32'49.20"	95°32'55.43"

Table 2. Water temperature analysis results.

Test	IS1 (°C)	IS2 (°C)	IS3 (°C)
Test 1	84.21	82.55	78.13
Test 2	84.26	82.54	78.09
Test 3	84.23	82.56	78.11
Mean	84.23	82.55	78.11
Std. Deviation	0.025	0.01	0.02

Table 3. FLIR temperature analysis.

Test	IS1 (°C)	IS2 (°C)	IS3 (°C)
Test 1	72.4	75.8	63.9
Test 2	61.7	70.5	68.5
Test 3	63.6	74.7	70.6
Mean	65.9	73.7	67.7
Std. Deviation	5.7	2.8	3.4

flown together with drones to detect the location of geothermal manifestations that FLIR had recorded. The image obtained through DEMNAS was then used to construct a 3D model through the ArcScene application to provide a more realistic picture of field conditions for future exploration missions.

3. Results and Discussions

3.1. Water Temperature Analysis

The results of the analysis of water temperature data can be seen in Table 2. It is known that the water temperature data at the IS1 test location has an average of 84.23°C from the three tests. For IS2, the average temperature is 82.55°C, and for IS3, the average temperature is 78.11°C. The standard deviation for each test is 0.025°C, 0.01°C, and 0.02 °C for IS1, IS2, and IS3, respectively. It can be seen that the highest water temperature is at the IS1 test location in test 2, with a value of 84.26 °C. The lowest temperature is at the IS3 test location in test 2, with a temperature of 78.09 °C.

3.2. FLIR Temperature Analysis

The results of the analysis of temperature obtained by FLIR can be seen in Table 3. It is known that the highest temperature is at the IS2 test location in test 1, with a temperature of 75.8 °C, and the lowest temperature is at the IS1 test location, with a temperature of 61.7 °C in Test 2. Based on all the temperatures obtained, it is also known that the average obtained at IS1 is 65.9°C, IS2 is 73.7°C, and IS3 is 67.7°C. The standard deviation for each point has also been identified, where the calculated standard deviation for IS1, IS2, and IS3 are 5.7°C, 2.8°C, and 3.4°C, respectively. The results obtained from the FLIR thermal camera, together with the surface temperature of the thermal features at the IS1, IS2, and IS3, can be seen in Figure 2.

Based on the data collection that has been carried out for each test location, the image scale can be calculated from the FLIR focus value and the drone height value of 1:100. The scale calculation is calculated using the formula Scale = Focus / Height, where the value is 15 cm / 15 m = 150 mm / 15000 mm = 1/100 or 1:100. Based on FLIR data collection, surface temperature values, and thermal images were obtained by the FLIR thermal camera when flown together with drone.

In this study, the thermal images show color variants ranging from bluish-black or purplish blue for the lowest temperature, and white for the highest temperature. The surface temperature value on the thermal pallet is taken based on the highest value obtained in this test, namely 75.8 °C. For thermal pallets with colors ranging from bluish-black or purplish-blue having temperature values ranging from35.8 °C, the orange color has a temperature value with a value range of 55.8 °C, and finally, for the white color, the temperature value range reaches 75.8 °C. The thermal temperature value in the image above refers to the thermal temperature value in the previously obtained thermal image.

3.3. Landsat 8 Satellite Image Temperature Analysis

Optical image data can provide preliminary results of geothermal features in the Ie Seu'um manifestation. However, because the data resolution from satellite images is very low, the response obtained at the manifestation location with a small area (50 x 50 m) is only represented by 3 pixels of data for the thermal band. Therefore, drones are used as a low-cost research method to study geothermal features in a relatively small area and study the safety of exploration in the Ie Seu'um manifestation. Figure 3 shows some of the processing results and composite bands on Landsat 8 data.

Landsat OLI/TIRS data is used to calculate (a) NDVI, (b) emissivity values obtained from NDVI calculations of vegetation propagation, where the data is also overlaid with safety paths and temperature contours obtained from temperature surface in band 10 for Landsat 8 data. Based on the results of processing surface temperature on Landsat 8 satellite imagery, we also overlay the temperature data from the thermal band analysis according to the NDVI response and emissivity, where the average surface temperature obtained is 30.3 °C in the area of manifestation.

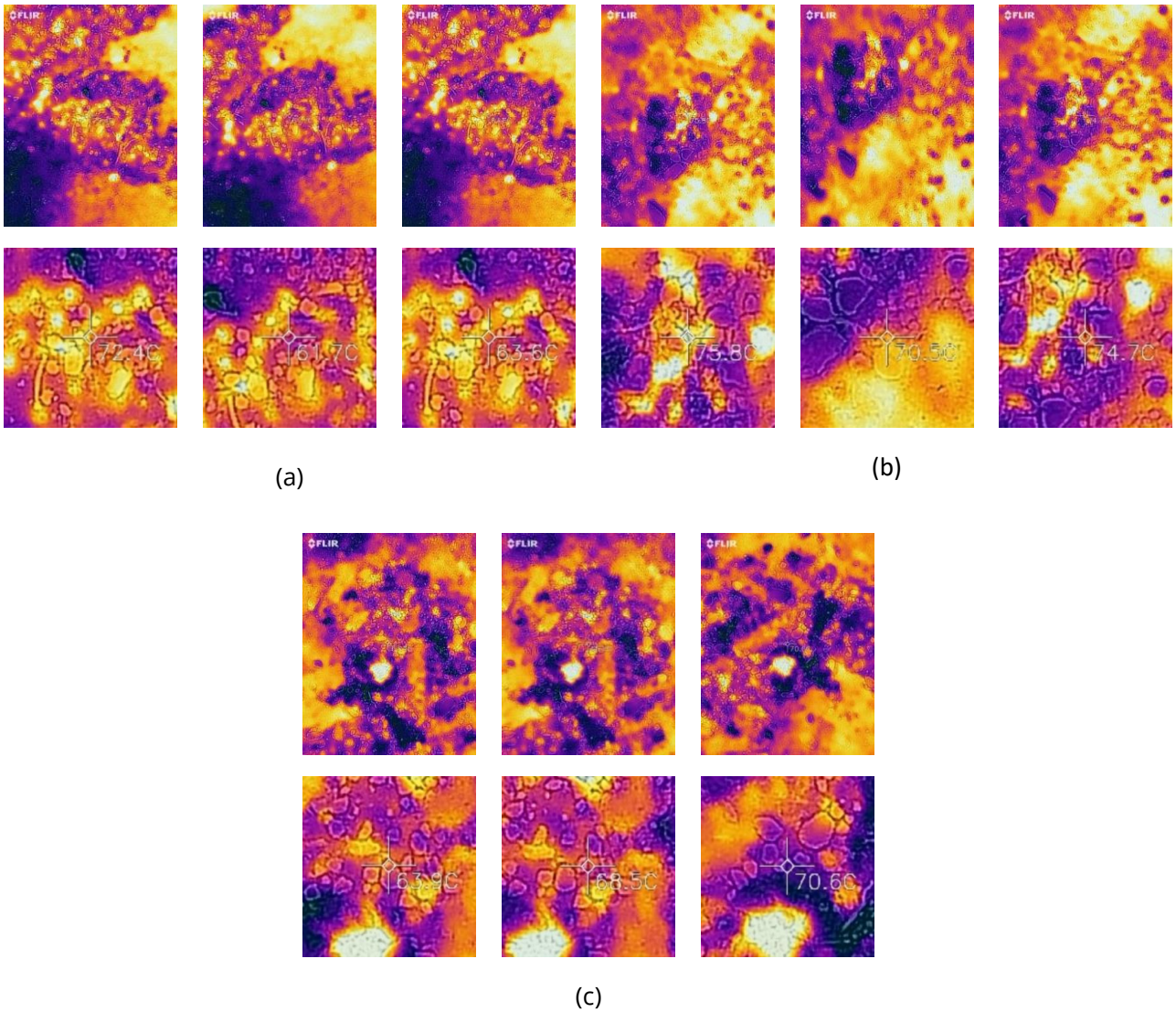

Figure 2. Test location for (a) IS1; (b) IS2; and (c) IS3.

For comparison, the average surface temperature values that have been obtained at predetermined test locations, such as IS1 of 31.7 °C, IS2 of 31.7 °C, and IS3 of 31.2 °C. For the standard deviation of the surface temperature, the value obtained is 0.7 °C. It is also known that the highest surface temperature and lowest surface temperature at each test location, where the highest temperature is at the IS1 and IS2 test locations with a temperature of 31.7 °C and the lowest temperature are at the IS3 test location with a temperature of 31.2 °C.

The hot temperature from the volcanic activity that occurred in the manifestation of Ie Seu'um made some plants unable to grow around the manifestation area. It should be noted that the area is not vegetated because of the volcanic activity that occurs beneath it and the agricultural activities carried out by the surrounding community. However, in several test locations, such as IS1, IS2, and IS3, it appears that these locations are vegetated around the thermal features, where the low NDVI values obtained indicate volcanic activity in the area. This happens because the surface emissivity data represents the ground surface's ability to convert heat energy into radiant energy so that the greater an object absorbs heat, the smaller the reflected radiation. These multispectral data yield the same vegetation distribution and emissivity response as Landsat 8 satellite data. From the results, it is known that the thermal temperature data from FLIR has a value that is closer to the temperature in water compared to the thermal data from the Landsat 8 satellite image. This proves that the temperature on FLIR is more accurate than the Landsat 8 temperature. This is because tropical regions such as Indonesia have optical satellite images that are often blocked by clouds, which can also be a trigger that the temperature obtained is not accurate.

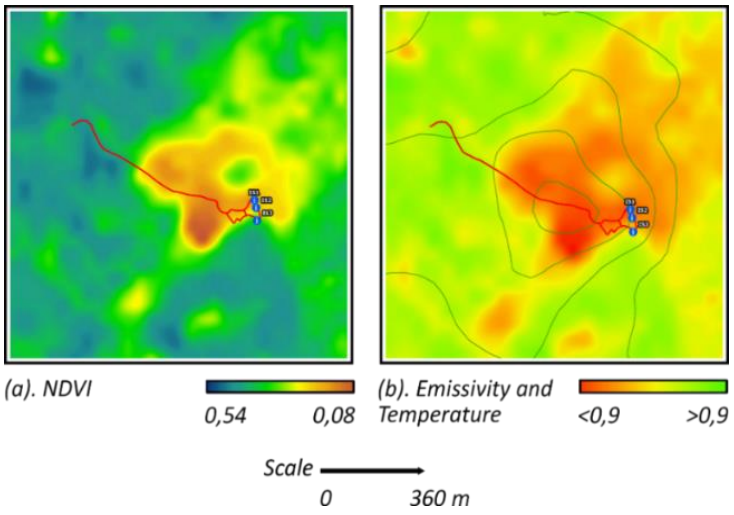

Figure 3. Analysis of satellite data at the location of the manifestation of Ie Seu'um (a) NDVI (b) Emissivity and temperature

3.4. Creating the DEM

The entire elevation value from the DEMNAS image is used to create the DEM map, but not all areas in the satellite imagery are processed for data. Only the area required with specific considerations is used in the study. This area is then selected for 3D map modeling after the exact model is made. Based on the image obtained from Avenza Maps, we can determine the security path to the location of the research point by using the path recording feature in the application. Using the ArcMap application, data from the Avenza application is processed to get a better map view regarding the security path of the exploration area. In Figure 4, we can see the appearance of the security path of the exploration area and the test location on the geothermal manifestation of Ie Seu'um. We can see that the security path is created using a polyline based on the actual path, representing the safest path to pass at the location of the Ie Seu'um geothermal manifestation. It can also be seen in the image above that the test locations are marked with a blue label with the names IS1, IS2, and IS3.

An elevation map of the geothermal manifestation of Ie Seu'um was made based on the cropped DEMNAS image to limit the research location and classification of altitude classes. The results of its manufacture produce 15 height classes. Ie Seu'um is an area with quite variable altitude values, where the range of elevation figures in this region has a value of 0 masl to more than 560 masl where it can be said that the Ie Seu'um geothermal manifestation area has varied land construction. Figure 5 shows the elevation map of the geothermal manifestation of Ie Seu'um.

Areas with red color have a value range of 400 masl – 560 masl more, in the range of class 11 and class 15. The yellow area has a value range of 200 masl – 400 masl, in the class range of 6 and 10. While the green areas have a value of 0 masl - 200 masl and are between classes 1 and 5.

It can be seen in Figure 6 below, which is a clearer view of the elevation map in displaying the security path and location coordinates for the Ie Seu'um geothermal manifestation. The 2D image of the manifestation of Ie Seu'um is overlaid with the DEMNAS image of the Ie Seu'um geothermal area to detect whether the path to the test location is a safe route to be traversed in terms of surface elevation aspects. The results show that the initial route is in the green area while the test location is in an area that is slightly uphill, so it places it in the yellow to the red area. It is not surprising why this happened because the predetermined test location for each point was at an altitude of 178 masl for IS1, followed by IS2 at an altitude of 179 masl, and for IS3 at an altitude of 142 masl. The higher the altitude class, the higher the vigilance that must be considered to maintain the safety of this research. In Figure 7, you can also see the appearance of the DEM Ie Seu'um map, which was built in 3D.

Based on the DEMNAS image, we also built a slope map for the Ie Seu'um geothermal manifestation. We classified the slope at the manifestation site into 12. The Ie Seu'um geothermal manifestation survey area is an area that has a slope value that varies with a slope value ranging from the flattest of 0° to the steepest of 45°. For information on the safety of the exploration area, it can be said that the gentler the slope, the lower the danger that can occur, but the steeper the slope, the higher the risk. In this case, the level of vigilance of the researchers should be higher during exploration missions to maintain the safety and security of all researchers. Figure 8 shows the map of the slope of the geothermal manifestation of Ie Seu'um. It can be seen that the slope of the test site is

Figure 4. Ie Seu'um geothermal manifestation exploration safety path

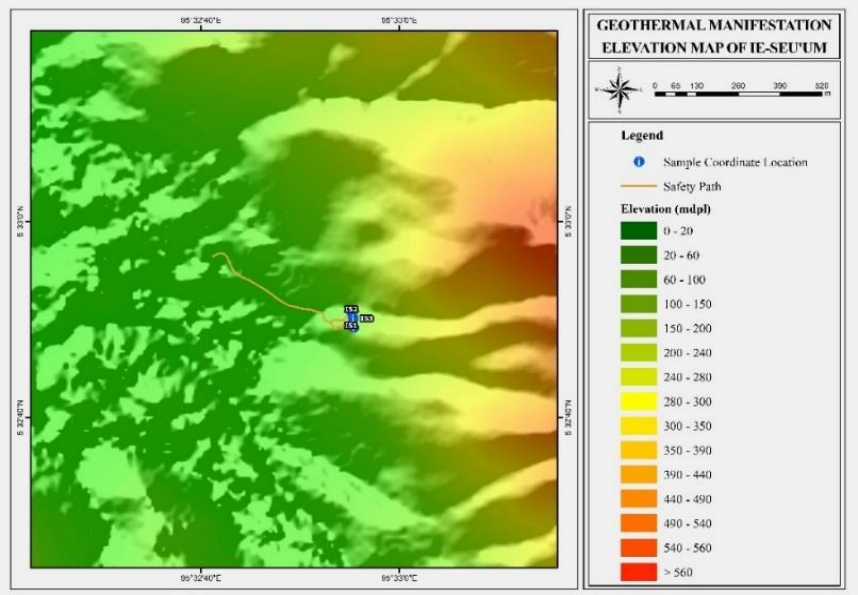

Figure 5. The elevation map of Ie Seu'um

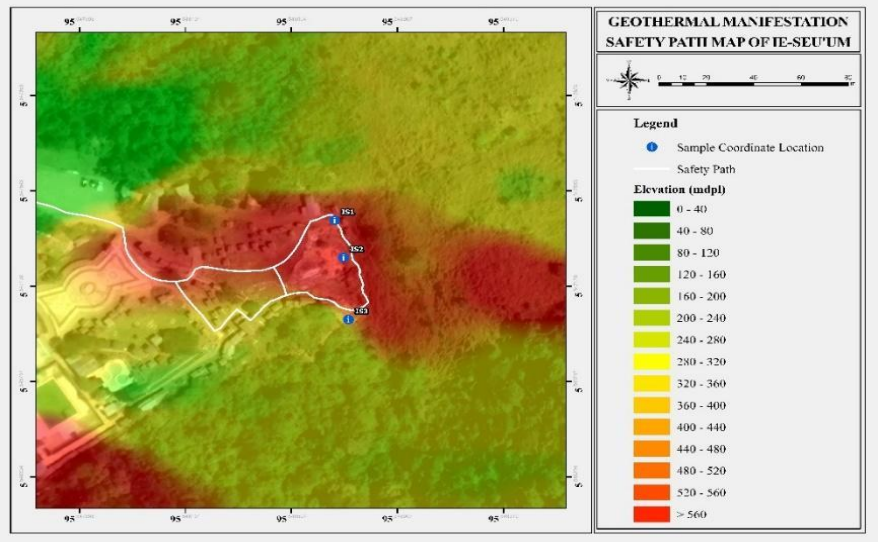

Figure 6. The safety path map of Ie Seu'um

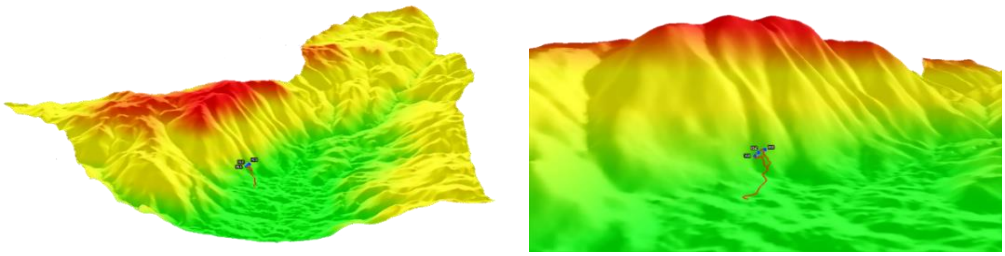

(a) (b)

Figure 7. (a) 3D imagery in the entire Ie Seu'um area (b) 3D image with a closer view

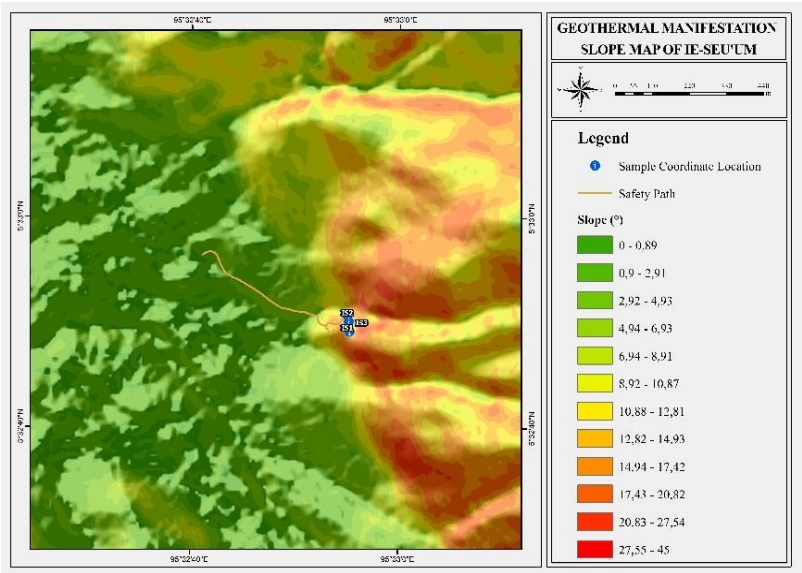

Figure 8. The slope map of Ie Seu'um

in the lower middle class, so the risk of dangerous threats from the research location is not too high. However, we must pay extra attention to how we collect water temperature data and FLIR thermal data since collecting these might get us to slip in hot water with the Ie Seu'um geothermal manifestation if we are not careful.

4. Conclusions

This study demonstrates the effectiveness of drones equipped with FLIR thermal cameras in identifying varying temperature values in relation to water temperature data, FLIR thermal temperature data, and temperature data from Landsat 8 satellite imagery. The results indicate that these drones are valuable tools for locating hot springs and thermal features in hard-to-reach areas like the Ie Seu'um manifestation location. Additionally, the study provides an estimation of the geothermal reservoir temperature based on the hot springs in the Ie Seu'um geothermal manifestation.

Acknowledgments: The authors express their gratitude to their individual institutions and universities.

Author Contributions: Conceptualization, R.A.B., T.R.N. and I.I.; methodology, R.A.B., G.M.I., R.S.; software, R.A.B., T.R.N. and M.Y.; validation, E.Y., N.N. and I.I.; formal analysis, R.A.B., G.M.I., R.S.; investigation, R.A.B., E.Y.; resources, R.A.B., M.Y.; data curation, M.Y., N.N.; writing—original draft preparation, R.A.B; T.R.N.; writing—review and editing, N.N., I. I.; visualization, G.M.I., R.S.; supervision, I.I.; project administration, N.N., I.I.; funding acquisition, I.I. All authors have read and agreed to the published version of the manuscript.

Funding: This study does not receive any external funding.

Ethical Clearance: Not applicable.

Informed Consent Statement: Not applicable.

Data Availability Statement: All data is available upon request to the corresponding author.

Conflicts of Interest: All the authors declare that there are no conflicts of interest.

References

1. Silitonga, A. S., Masjuki, H. H., Mahlia, T. M. I., Ong, H. C., Chong, W. T., Boosroh, M. H. (2013). Overview properties of biodiesel diesel blends from edible and non-edible feedstock, *Renewable and Sustainable Energy Reviews*, Vol. 22, 346–360
2. Idroes, R., Yusuf, M., Saiful, S., Alatas, M., Subhan, S., Lala, A., Muslem, M., Suhendra, R., Idroes, G. M., Marwan, M., Mahlia, T. M. I. (2019). Geochemistry Exploration and Geothermometry Application in the North Zone of Seulawah Agam, Aceh Besar District, Indonesia, *Energies*, Vol. 12, No. 23, 4442. doi:10.3390/en12234442
3. Idroes, R., Yusuf, M., Alatas, M., Lala, A., Suhendra, R., Idroes, G. M. (2019). Geochemistry of Sulphate spring in the Ie Jue geothermal areas at Aceh Besar district, Indonesia, *IOP Conference Series: Materials Science and Engineering* (Vol. 523), IOP Publishing, 12012
4. Idroes, R., Yusuf, M., Alatas, M., Subhan, Lala, A., Muslem, Suhendra, R., Idroes, G. M., Suhendrayatna, Marwan, Riza, M. (2019). Geochemistry of warm springs in the Ie Brôuk hydrothermal areas at Aceh Besar district, *IOP Conference Series: Materials Science and Engineering*, Vol. 523, 012010. doi:10.1088/1757-899X/523/1/012010
5. Idroes, R., Yusuf, M., Alatas, M., Lala, A., Suhendra, R., Idroes, G. M. (2018). Geochemistry of hot springs in the Ie Seu'um hydrothermal areas at Aceh Besar district, Indonesia, *IOP Conference Series: Materials Science and Engineering* (Vol. 334), IOP Publishing, 12002
6. Idroes, G. M., Syahnur, S., Majid, S. A., Sasmita, N. R., Idroes, R. (2021). Provincial economic level analysis in Indonesia based on the geothermal energy potential and growth regional domestic products using cluster analysis, *IOP Conference Series: Materials Science and Engineering* (Vol. 1087), IOP Publishing, 12079
7. Nasruddin, Idrus Alhamid, M., Daud, Y., Surachman, A., Sugiyono, A., Aditya, H. B., Mahlia, T. M. I. (2016). Potential of geothermal energy for electricity generation in Indonesia: A review, *Renewable and Sustainable Energy Reviews*, Vol. 53, 733–740. doi:10.1016/j.rser.2015.09.032
8. Idroes, G. M., Maulana, A., Suhendra, R., Lala, A., Karma, T., Kusumo, F., Hewindati, Y. T., Noviandy, T. R. (2023). TeutongNet: A Fine-Tuned Deep Learning Model for Improved Forest Fire Detection, *Leuser Journal of Environmental Studies*, Vol. 1, No. 1, 1–8. doi:10.60084/ljes.v1i1.42
9. Wibowo, K. M. W. M., Kanedi, I., Jumadi, J. (2015). Geographic Information System (GIS) Determines Coal Mining Locations in Bengkulu Province Based on a Website, *Jurnal Media Infotama*, Vol. 11, No. 1
10. Hariyanto, T., Robawa, F. N. (2016). Identification of geothermal potential using landsat 8 and location determination of geothermal power plants (Case Study: Mount Lawu Area), *Geoid*, Vol. 12, No. 1, 36–42
11. Indarto, I., Prasetyo, D. R. (2014). Generation of 10m Resolution Digital Elevation Model from RBI Map and GPS Survey with ANUDEM Algorithm, *Jurnal Keteknikan Pertanian*, Vol. 2, No. 1
12. Utomo, B. (2018). Drones for Accelerated Mapping of Land Planes, *Media Komunikasi Geografi*, Vol. 18, No. 2, 146. doi:10.23887/mkg.v18i2.12798
13. Hamur, P. K. (2019). Study of Aerial Photo Data Processing Using Agisoft Photoscan and Pix4dmapper Software (Case Study: Lowokwaru District, Malang City), ITN MALANG
14. Uysal, M., Toprak, A. S., Polat, N. (2015). DEM generation with UAV Photogrammetry and accuracy analysis in Sahitler hill, *Measurement*, Vol. 73, 539–543
15. Marwan, Noviandy, T. R., Maulana, A., Suhendra, R., Yusuf, M., Lala, A., Idroes, G. M., Muslem, Mahmudi, Idroes, R. (2021). Utilization of unmanned aerial vehicles in geothermal exploration: A review, *IOP Conference Series: Materials Science and Engineering* (Vol. 1087), IOP Publishing, 12072
16. Cherkasov, S. V., Farkhutdinov, A. M., Rykovanov, D. P., Shaipov, A. A. (2018). The Use of Unmanned Aerial Vehicle for Geothermal Exploitation Monitoring: Khankala Field Example, *Journal of Sustainable Development of Energy, Water and Environment Systems*, Vol. 6, No. 2, 351–362. doi:10.13044/j.sdewes.d6.0196
17. Bjornsson, G., Grímsson, G., Sigurdsson, A., Laenen, V. (2019). *Thermal Mapping of Icelandic Geothermal Surface Manifestations with a Drone*
18. Walter, T. R., Jousset, P., Allahbakhshi, M., Witt, T., Gudmundsson, M. T., Hersir, G. P. (2020). Underwater and drone based photogrammetry reveals structural control at Geysir geothermal field in Iceland, *Journal of Volcanology and Geothermal Research*, Vol. 391, 106282. doi:10.1016/j.jvolgeores.2018.01.010
19. Harvey, M. C., Rowland, J. V., Luketina, K. M. (2016). Drone with thermal infrared camera provides high resolution georeferenced imagery of the Waikite geothermal area, New Zealand, *Journal of Volcanology and Geothermal Research*, Vol. 325, 61–69. doi:10.1016/j.jvolgeores.2016.06.014
20. Marwan, Idroes, R., Yanis, M., Idroes, G. M., Syahriza. (2021). A low-cost UAV based application for identify and mapping a geothermal feature in ie jue manifestation, Seulawah Volcano, Indonesia, *GEOMATE Journal*, Vol. 20, No. 80, 135–142